Fachtagung "Experimentelle Strömungsmechanik"
3. – 5. September 2019, Erlangen

Entwicklung von faser-optischen Drucksensoren für die Verwendung in instationären Mehrlochsonden

Development of Fiber-Optic Pressure Sensors for the Usage in Unsteady Multi-Hole Probes

Florian M. Heckmeier[1*], Korbinian Meusel[1], Sascha Kienitz[2], Daniel Iglesias[3], Christian Breitsamter[1]
[1] Technische Universität München, Fakultät für Maschinenwesen,
Lehrstuhl für Aerodynamik und Strömungsmechanik
Boltzmannstr. 15, 85748 Garching bei München, [*] E-Mail: florian.heckmeier@aer.mw.tum.de

[2] fos4X GmbH, Thalkirchner Str. 210, 81371 München

[3] Vectoflow GmbH, Friedrichshafener Str. 1, 82205 Gilching

Mehrlochsonden, faser-optische Sensoren, instationäre Druckmessung, Fabry-Pérot
multi-hole probe, fiber-optic sensor, unsteady pressure measurement, Fabry-Pérot

Abstract

When measuring unsteady flow phenomena with multi-hole pressure probes, the sensors are integrated inside the probe near the probe tip. Arbitrary outer shapes of the probes can be realized with the additive manufacturing process *selective laser melting* (SLM). In order to realize multi-hole probes with higher temporal resolution, which can be operated in harsh environments, a fiber-optic sensor is developed. The sensor is built out of two micromachined fused silica (SiO_2) wafers, which are bonded together. The sensor is operated differentially with a pressure capillary by either pressurizing the sensor or using the surrounding static pressure as the reference pressure. The measurement principle of the fiber-optic sensor is based on the Fabry-Pérot interferometer effect. The cylindrical sensor's diameter and depth is 2 mm, respectively. For the quantification of the sensor measurement capabilities, various validation tests have been performed: Besides a static and dynamic calibration, comparisons with a state-of-the-art piezo-resistive pressure sensor have been performed. The focus lies on the reproducibility of both frequency response and amplitude. The linear pressure range, the sensor resolution and the cross-sensitivities are determined. The signal-to-noise ratio of the whole measurement chain is compared to a state-of-the-art piezo-resistive sensor measurement chain. Furthermore, the acoustic transfer function of a silicone tube is analyzed experimentally in a frequency test-rig and is compared to an analytical solution.

Introduction

Highly fluctuating flow fields occur in turbomachinery due to interactions of rotating and non-rotating components. These sources of unsteadiness have to be understood either by means

GALA e.V., Karlsruhe, Germany, ISBN 978-3-9816764-6-4

of numerical simulations or experimental measurements. Even though sophisticated CFD simulations enable an insight in unsteady flow phenomena inside turbo machines, it is evident that experimentally gained results are still of great interest for both, academic and industrial research. Furthermore, experimental results can be used for the validation of newly implemented CFD-approaches. In addition, by installing probes with high bandwidths inside turbines, live monitoring of the unsteady flow is possible.
In principle, measurement methods can be divided into intrusive and non-intrusive/optical techniques. Optical measurement methods, like particle image velocimetry (PIV) or laser Doppler anemometry (LDA), can be used to determine the velocity field. However, optical accessibility, a rather time consuming calibration and significant set up costs are the disadvantages of non-intrusive methods.
Pressure probes and hot-wire probes are the most represented intrusive techniques. Hot-wires feature high temporal resolution but lack of robustness in harsh environments. In contrast, pressure probes are more cost-efficient and easy to use. Since the 1990s research institutes worldwide developed unsteady multi-hole probes, enlarging their abilities and ensuring their use in different measurement scenarios (see Humm et al. 1995, Ainsworth et al. 2000, Rediniotis et al. 1999). However, spatial and temporal resolution and the temperature resistance are still a major focus of research efforts.
By conducting spatial and temporal calibrations in order to describe the aerodynamic and dynamic behavior of the pressure probe in a flow field, accurate measurements can be ensured. While flush mounted pressure transducers have optimal dynamic response, they experience high loads, increase the size of probe tip geometries and, therefore, result in larger intrusive influence of the probe. This problem can be counteracted by either miniaturizing the sensors or placing the sensors farther inside the pressure probe (see Grimshaw and Taylor 2017). However, the latter solution requires a characterization of the acoustic channel system and a reconstruction of the flow quantities at the probe tip (see Rediniotis et al. 2003).
State-of-the-art measurements of highly dynamic, unsteady pressure flow fields are mostly conducted with electrical transducers. However, those transducers show disadvantages regarding cross-sensitivities against electro-magnetic distortions and the need for active power supply of the electrical components. Depending on the measuring principle, the electrical sensors can be divided into resistive, piezo-resistive, capacitive and piezo-electric sensors. In order to exceed limitations of conventional electrical pressure transducers, optical sensor principles can be applied. Previous developments resulted in durable pure glass fiber-optic sensors for surface pressure measurements (see Schmid et al. 2016, Schmid et al. 2017).
The goal of the cooperation project between the sensor specialist fos4X GmbH, the pressure probe manufacturer Vectoflow GmbH and the Chair of Aerodynamics and Fluid Mechanics of the TU Munich is to demonstrate a new approach on the usage of the optical theory in order to have a differentially operated pressure sensor in cylindrical form. The sensor should be appropriate for the installation and usage in unsteady multi-hole pressure probes. This paper describes the main steps towards such kind of sensors in additive manufactured unsteady multi-hole probes. First, the design, manufacturing and calibration process of miniature pressure probes is discussed. Second, the development and the theoretical fundamentals of fiber-optic sensors are given. In the last part of the paper, experimental investigations which show the characteristics and potential improvements of the sensor are conducted.

Design of an Unsteady Multi-Hole Probe

The cooperation partners aim for the development of unsteady multi-hole probes (see Figure 1) using fiber-optic pressure transducers. Application scenarios for such probes can be in aer-

GALA e.V., Karlsruhe, Germany, ISBN 978-3-9816764-6-4

odynamic wind tunnels, as they occur in industry or at research institutes, and in turbomachinery. Therefore, differential unsteady pressure transducers are installed inside the probe. In turbomachinery, where signal frequencies are determined by multiples of the blade-passing frequency ($n \cdot f_{BPF} > 10\ kHz$), the enhancement of the temporal characteristic is the key driver of future developments. Intrusive effects can be counteracted by miniaturizing the probe and hence, make the probe more competitive to non-intrusive measurement techniques, like LDA or PIV. Moreover, by the usage of additive manufacturing arbitrary probe shapes can be realized. In the following section, the manufacturing, the spatial and temporal calibration, and the assembly of the probe are explained.

Figure 1: 3D-printed straight unsteady five-hole pressure probe and numeration of holes

For the construction of the arbitrary shaped probe head, the *selective laser melting* (SLM) method is used. This technology includes melting and sintering of materials for aerodynamic purposes, like metal and ceramic powders. In the post manufacturing cutting process, details in the outer shape can be realized. Thereby, e.g. different probe tip geometries can be achieved with a high surface quality (see Figure 2).

Figure 2: 3D-printed L-shaped probe head: After 3D-printing (left) and after post manufacturing (right)

Every probe has to be calibrated in a known environment before using it in a free-field experiment, where the flow conditions in terms of flow angles, velocity and pressure magnitude are unknown. In contrast to steady multi-hole probes, which solely require a spatial/angular calibration, unsteady pressure probes additionally need the characterization of the acoustic system inside the pressure channels in a temporal/dynamic calibration process. A brief description of both, the spatial and the temporal calibration, is given in the following:
In the spatial calibration, the correlation between the mean free-stream flow conditions and the measured pressures is determined. In the free-jet calibration wind tunnel facility, the free-stream velocity U_∞ and the flow angles α and β are set, the corresponding pressures $p_1, p_2, \dots, p_5$ at the five pressure ports (see Figure 1) measured and stored in non-dimensional post-processed look-up tables. In the literature, various methods are documented on how the calibration data is used for the reconstruction of the flow-field properties at the probe tip, when measuring in unknown flows (see Johansen et al. 2001). Predominantly, interpolation schemes are used to process the non-dimensional pressure calibration coefficients. Besides local and global interpolation schemes, neural-network approaches are also investigated. Depending on

GALA e.V., Karlsruhe, Germany, ISBN 978-3-9816764-6-4

the calibration grid density, the number of calibrated velocities and the accuracy of the reconstruction algorithms, absolute angular errors and the deviation of the calculated velocity are aimed to be below 1° and 1 m/s or with a relative error smaller than 1%, respectively.
The channels inside the probe, which are located between the probe tip and the pressure transducers mainly determine the temporal characteristics of the probe. Therefore, this acoustic system, which is primarily dominated by the channel's length L, the diameter d and the volume directly in front of the sensor V (see Figure 3) , can either be approximated by analytical functions (see Bergh and Tijdeman 1965) or determined in an experimental test-rig. The complex ratio $H(\omega) = p_{tip}/p_{sensor}$ describes the attenuation and phase shift for the acoustic propagation inside the acoustic system depending on the signal frequency. In the frequency test-rig which consists of an amplifier, a speaker and an acoustic test chamber, the test object and a reference sensor are installed in close proximity. Sinusoidal signals of multiple frequencies with a specified frequency step size are emitted by the speaker and the amplitude ratio and phase shift between the sensors inside the test object and the reference sensor are determined.

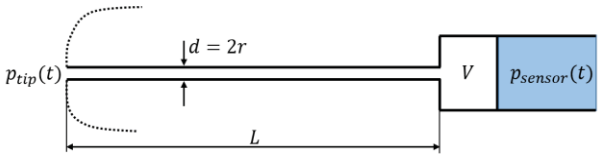

Figure 3: Sketch of the tubing inside the probe from the probe tip to the location of the sensor

By applying the transfer function to the Fourier transformed pressure signal, the temporal characteristics of the probe can be taken into account and, hence, the pressure at the tip is reconstructed:

$$P_{tip}(\omega) = H(\omega)P_{sensor}(\omega) \qquad (1)$$

In the following, design aspects and properties of the conventional unsteady pressure probe are discussed and summarized in Table 1. It should serve as a preliminary design and state-of-the-art solution, where the newly developed fiber-optic sensors could be inserted easily in the future. The straight five-hole probe is manufactured with the SLM process. The hemispheric tip and the cavities, in which the sensors are installed, are post manufactured by cutting/drilling. The shaft diameter is mainly limited by the sensor size. For this unsteady probe five piezo-resisitve Meggitt Endevco 8507C-2 transducers are pressed into the drilled cavities with a surrounding silicone tubing in order to prevent leakage (see Meggitt Endevco 2018). The spatial calibration ensures reconstructions of flow angles up to $\pm$45°. The temporal calibration yields a transfer function for each channel. Signal frequencies up to 10 kHz can be resolved and reconstructed.

Table 1: Multi-hole probe properties incl. calibration specifications

Probe / tip shape	Straight / hemispheric
Tip diameter	$3\ mm$
Shaft diameter	$15\ mm$
No. channels/holes	5
Channel diameter	$\leq 1\ mm$
Sensor type	Meggitt Endevco 8507C-2
Sensor diameter	$2.3\ mm$
Spatial calibration	$\pm 45°$
Temporal calibration	$10\ kHz$

GALA e.V., Karlsruhe, Germany, ISBN 978-3-9816764-6-4

Development of a Fiber-Optic Sensor

The newly developed fiber-optic sensor at the end of a standard telecommunication fiber works similar to their electrical counterparts. The fiber-optic sensor is constructed as a passive MEMS glass chip and is based on the principles of the so-called Fabry-Pérot interferometer. It consists of a diaphragm/membrane, a resonance cavity and two mirrors (see Figure 4). The end of the fiber and the inner part of the membrane represent the two mirrors.

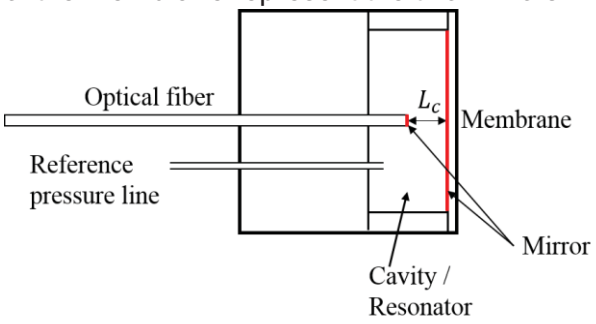

Figure 4: Schematic sketch of the fiber-optic pressure sensor

The applied pressure p bends the diaphragm and changes the cavity length L_c between the two mirrors. The sensitivity of the transducer is predominantly characterized by the mechanical displacement of the membrane. The maximum deflection ΔL of the diaphragm can be calculated as a function of the applied pressure p (see Schmid et al. 2017):

$$\Delta L = \frac{3r^4(1-\nu^2)}{16Eh^3} \cdot p \qquad (2)$$

Hereby, E is the Young's modulus, ν the Poisson's ratio, and r and h radius and thickness of the sensor membrane. A broadband light travels through the fiber-optic cable and optical interference modulates the light spectrum inside the cavity depending on the cavity length. An increasing cavity length shifts the phase condition of the destructively interfered wavelength in the spectrum to larger wavelengths, while a smaller cavity length shifts the spectrum to smaller wavelengths (see Schmid et al. 2016, Yin et al. 2014). By adjusting the distance between the fiber and the diaphragm, the reflected spectrum of the sensor can be matched to the operating point (Q-point) of an edge-filter interrogator. Hence, a single destructive interference is filtered by the edge-filter. The modulated light is guided back by the same fiber to the measurement device which contains two photodiodes. While one part of the light is focused directly on a photodiode, the other part is optically filtered and linked on a second photodiode afterwards. The ratio of the light intensities reveals the phase shift of the reflected spectrum depending on the applied pressure. Cross-sensitivities to fiber bending, transmission loss and fluctuations of the optical light power are not taken into account. Due to the absence of conductive materials, the sensor is inherently immune to electric-magnetic interference, robust against water, humidity and corrosion. The optical filtering process ensures sampling rates of up to $f_s = 50\ kHz$. The sensor is built out of two micromachined fused silica (SiO_2) wafers, which are bonded together. Further information regarding the selective laser etching (SLE) bonding process is given in Ref. LightFab 2019. The sensor is operated differentially with a pressure capillary by either pressurizing the sensor or using the surrounding static pressure as the reference pressure. In order to have a mirror surface at the diaphragm, which only allows reflection of the light inside the cavity, the outer membrane surface is optically terminated.

GALA e.V., Karlsruhe, Germany, ISBN 978-3-9816764-6-4

Experimental Setup and Results

In Figure 5, a fiber-optic sensor of the 1st generation is displayed besides a 1-Cent coin for a qualitative size comparison. All experimental tests are conducted with ten sensors of this kind. Tests include the determination of the calibration coefficient, temperature sensitivities and comparisons to piezo-resistive sensors.

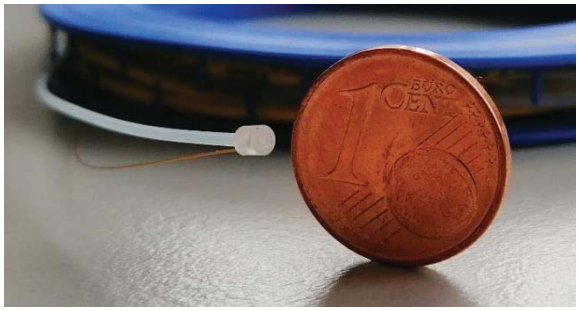

Figure 5: Differential pressure transducer: qualitative size comparison

In the calibration process, the correlation between the optic output value ρ_{opt} and the applied pressure p is determined for the linear pressure range by $p = \rho_{opt} \cdot k^{-1}$. By applying predefined pressures, either statically or dynamically, the calibration coefficient k is calculated. Tests show that the calibration of the sensor strongly depends on the ambient conditions and the installation situation. Therefore, it is important to know the influence of these limiting conditions during calibration and to separate them in the best possible way. Temperature resistance is limited due to the use of adhesive when attaching the optical fiber and the pressure capillary to the ferrule. In addition, the temperature sensitivities vary from sensor to sensor, but behave linearly. For a first comparison of the dynamic behavior of the new fiber-optic sensor to a state-of-the-art piezo-resistive sensor, the sensors are placed next to each other in the frequency test-rig. Sinusoidal excitations in the frequency range of $f_s = [100, 1000]\ Hz$ are measured and compared. The signal frequencies are exactly reproduced by both sensor types with relative errors smaller than 1% in the whole frequency range. Figure 6 shows the pressure amplitudes measured by both sensors. Furthermore, the relative deviation of the fiber-optic sensor to the piezo-resistive sensor is depicted. It can be observed that the amplitudes also match very well. Larger errors at $f_s = \{100, 400\}\ Hz$ could be due to acoustic modes in the frequency test-rig, that have been observed in previous measurements as well.

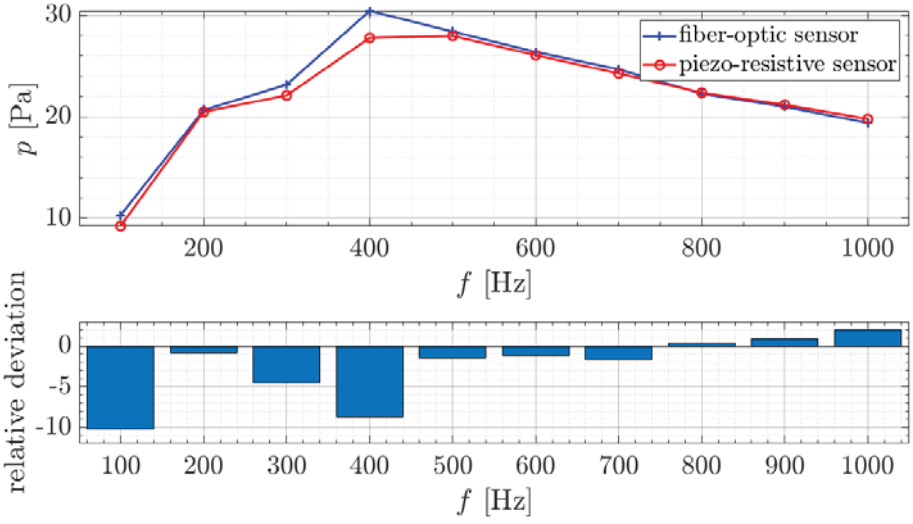

Figure 6: Pressure amplitudes of a fiber-optic sensor placed next to a piezo-resistive sensor in the frequency test-rig dependent on the excitation frequency

GALA e.V., Karlsruhe, Germany, ISBN 978-3-9816764-6-4

Tests regarding the noise level are conducted: The measurement chain of the piezo-resistive sensor connected to NI 9237 modules show better signal-to-noise ratios (SNR) than the fiber-optic sensor. This is due to the lack of enhanced signal conditioning in the optic measurement acquisition. The optic measurement chain is still under development and efforts concerning bandwidth and noise specifications have to be addressed by changes in hardware.
In order to test the fiber-optic sensor in a more realistic application, the transfer function of a silicone tubing with $L = 200\,mm$ and $d = 1.5\,mm$ is determined in the aforementioned frequency test-rig. Variations of the combination of the reference sensor and the sensor at the end of the tubing are compared. The frequency step size is $20\,Hz$ and $100\,Hz$ for the piezo-piezo and optic cases, respectively. Moreover, the analytical solution by Bergh and Tijdeman is shown in Figure 7, where only the attenuation $\hat{p}_{tube}/\hat{p}_{ref}$ is displayed. For both cases, where the fiber-optic sensor is mounted at the end of the tubing, the resonance frequencies match the ones of the analytical and the piezo-piezo solution, which can be seen as the state-of-the-art and validated solution.

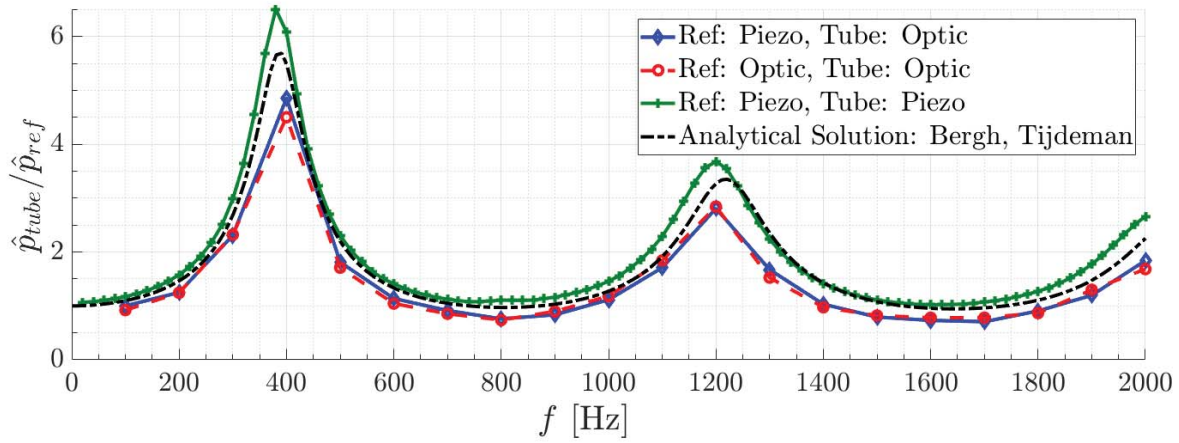

Figure 7: Attenuation $\hat{p}_{tube}/\hat{p}_{ref}$ for a silicone tubing with geometric parameters $L = 200\,mm$ and $d = 1.5\,mm$

The qualitative trend is reproduced very well, however, the amplitudes of the attenuation are underpredicted. A possible reason for this behavior is a systematic error, which can be attributed to a modification of the operating point of the sensor. The fiber-optic sensor is deformed by the surrounding silicone tubing marginally but sufficient enough to cause a change in the calibration coefficient. This leads to the conclusion that the assembly of the sensor into a test object is crucial regarding its behavior and therefore has to be addressed in the future carefully.

Conclusion

In this paper, the development of fiber-optic differential pressure sensors is shown. Beside an introduction to unsteady multi-hole probe measurement systems, details on the optic theory are given. Preliminary tests with the fiber-optic sensors of the 1st sensor generation already show good dynamic behavior and appropriate specifications in comparison to state-of-the-art sensors. Finally, in Table 2, a short comparison of the optimal fiber-optic sensor specifications of the 1st generation sensors to the Meggitt Endevco piezo-resistive sensor, which has been installed in an unsteady probe, is shown.

GALA e.V., Karlsruhe, Germany, ISBN 978-3-9816764-6-4

Table 2: Comparison of the fiber-optic sensor specifications to the state-of-the-art piezo-resistive transducer

		Fiber-optic sensor	Meggitt Endevco 8507C-2
Dimensions (diameter × depth)	$[mm \times mm]$	2.0×2.0	2.3×12.7
Pressure range	$[kPa]$	100	14
Maximum operating temperature	$[°C]$	120	107
Resonance frequency	$[kHz]$	290	70

In future developments further investigations have to be carried out, which focus on the temperature cross-sensitivity and maximum operating temperature. Furthermore, the determination of the dependence of the sensor calibration specifications on the assembly in test objects and the reproducibility of the sensor assembly to achieve sensor specifications comparable to state-of-the-art sensors are challenging goals. Supplementary improvements concerning signal conditioning within the optical measurement chain are of interest as well.

Acknowledgments

The authors would like to thank the German Federal Ministry for Economic Affairs and Energy for the funding of the project within the ZIM-program (Zentrales Innovationsprogramm Mittelstand, ZIM: ZF4037204WM6).

Literature

Ainsworth, R.W., Miller, R.J., Moss, R.W., Thorpe, S.J., 2000: “Unsteady pressure measurement”, Measurement Science and Technology, Vol. 11, No.7, pp. 1055–1076

Bergh, H., Tijdeman, H., 1965: "Theoretical and experimental results for the dynamic response of pressure measuring systems", NLR-TR F.238

Grimshaw, S.D., Taylor, J.V., 2017: “Fast Settling Millimetre-Scale Five-Hole Probes”, In ASME Turbo Expo 2016, pp. 1–13

Humm, H.J., Gossweiler, C.R., Gyarmathy, G., 1995: “On Fast-Response Probes: Part 2 - Aerodynamic Probe Design Studies”, Journal of Turbomachinery, Vol. 117, No. 4, p. 618

Johansen, E., Rediniotis, O., Jones, G., 2001: “The Compressible Calibration of Miniature Multi-Hole Probes”, Journal of Fluids Engineering, Vol. 123, No. 1, pp. 128-138

LightFab GmbH, 2019: Products & Technology, https://www.lightfab.de/, accessed on 2019-05-09

Meggitt Endevco, 2018: Datasheet Model 8507C-2, Meggitt (Orange County), Inc.

Rediniotis, O., Johansen, E., Tsao, T., Seifert, A., Pack, L., 1999: “MEMS-based probes for velocity and pressure measurements in unsteady and turbulent flowfields”, In 37th Aerospace Sciences Meeting and Exhibit, no. c, AIAA

Rediniotis, O., Allen, R., Zeiger, M., Johansen, E., 2003: “Embedded-Sensor, Fast-Response Multi-Hole Probes”, In 41st Aerospace Sciences Meeting and Exhibit, AIAA

Schmid, M., Müller, M., Kuhnle, B., Bauer, M., Pongratz, R., Altmikus, A., 2016: “Fiber optic acoustic pressure sensor with high dynamic range and low noise”, In Proceedings of the ETC 2016 - 36th European Telemetry and Test Conference, Nürnberg

Schmid, M., Kuhnle, B., Kienitz, S., Napierala, C., Scheit, C., Altmikus, A., Müller, M., Koch, A., 2017: “A fiber-optic sensor for measuring quasi-static and unsteady pressure on wind energy converters”, 4SMARTS-Symposium, Braunschweig

Yin, J., Liu, T., Jiang, J., Liu, K., Wang, S., Qin, Z., Zou, S., 2014: “Batch-producible fiber-optic Fabry-Pérot sensor for simultaneous pressure and temperature sensing”, IEEE Photonics Technology Letters, Vol. 26, No. 20, pp. 2070–2073

GALA e.V., Karlsruhe, Germany, ISBN 978-3-9816764-6-4